



NRL/FR/7320--00-9699

# Validating a Coupled Suite of Wave, Tide, and Surf Models at Onslow Bay, North Carolina

RICHARD A. ALLARD  
Y. LARRY HSU

*Ocean Dynamics and Prediction Branch  
Oceanography Division*

JANE MCKEE SMITH

*Coastal and Hydraulics Laboratory  
U.S. Army Corps of Engineers  
Engineering Research and Development Center, Vicksburg, MS*

KELLEY MILES

*Sverdrup Technology, Inc.  
Stennis Space Center, MS*

March 22, 2000

# REPORT DOCUMENTATION PAGE

*Form Approved*  
**OMB No. 0704-0188**

Public reporting burden for this collection of information is estimated to average 1 hour per response, including the time for reviewing instructions, searching existing data sources, gathering and maintaining the data needed, and completing and reviewing this collection of information. Send comments regarding this burden estimate or any other aspect of this collection of information, including suggestions for reducing this burden to Department of Defense, Washington Headquarters Services, Directorate for Information Operations and Reports (0704-0188), 1215 Jefferson Davis Highway, Suite 1204, Arlington, VA 22202-4302. Respondents should be aware that notwithstanding any other provision of law, no person shall be subject to any penalty for failing to comply with a collection of information if it does not display a currently valid OMB control number. **PLEASE DO NOT RETURN YOUR FORM TO THE ABOVE ADDRESS.**

<b>1. REPORT DATE (DD-MM-YYYY)</b> March 24, 2000		<b>2. REPORT TYPE</b> Final		<b>3. DATES COVERED (From - To)</b>	
<b>4. TITLE AND SUBTITLE</b>  Validating a Coupled Suite of Wave, Tide, and Surf Models at Onslow Bay, North Carolina				<b>5a. CONTRACT NUMBER</b>	
				<b>5b. GRANT NUMBER</b>	
				<b>5c. PROGRAM ELEMENT NUMBER</b>	
<b>6. AUTHOR(S)</b>  Richard A. Allard, Y. Larry Hsu, Jane McKee Smith,* and Kelley Miles <sup>†</sup>				<b>5d. PROJECT NUMBER</b>	
				<b>5e. TASK NUMBER</b>	
				<b>5f. WORK UNIT NUMBER</b>	
<b>7. PERFORMING ORGANIZATION NAME(S) AND ADDRESS(ES)</b>  Naval Research Laboratory Oceanography Division Stennis Space Ctr, MS 39529-5004				<b>8. PERFORMING ORGANIZATION REPORT NUMBER</b>  NRL/FR/7320--00-9699	
<b>9. SPONSORING / MONITORING AGENCY NAME(S) AND ADDRESS(ES)</b>  DoD Washington Headquarters Services Installation Accounting Division 1155 Defense Pentagon, Room BB269 Washington, DC 20301-1155				<b>10. SPONSOR/MONITOR'S ACRONYM(S)</b>	
				<b>11. SPONSOR/MONITOR'S REPORT NUMBER(S)</b>	
<b>12. DISTRIBUTION / AVAILABILITY STATEMENT</b>  Approved for public release; distribution is unlimited.					
<b>13. SUPPLEMENTARY NOTES</b> <sup>*</sup> Coastal and Hydraulics Laboratory, U.S. Army Corps of Engineers, Engineering Research and Development Center, Vicksburg, MS <sup>†</sup> Sverdrup Technology, Inc. Stennis Space Center, MS 39529					
<b>14. ABSTRACT</b>  In this study a suite of off-the-shelf wave, tide, and surf models are coupled to produce a physically consistent dynamic representation of the surf zone for Onslow Beach, North Carolina. Many of the models used in this study have undergone some degree of validation, however, the suite of models has not been evaluated. The Integrated Ocean Program (IOP) model suite consists of the deep-water wave model WAM, two shallow-water wave refraction models: (1) STWAVE and (2) REFDIF, the ADCIRC model which predicts water elevations and depth-averaged currents, and SURF96, an R&D version of the Navy Standard Surf Model. To evaluate the IOP suite of models, a series of oceanographic instruments were deployed in shallow water at Onslow Beach to measure wave heights, wave periods, and tidal elevations. Wave and tide measurements were collected during the Joint Task Force Exercise (JTFEX 97-3) for the period 28 August – 5 September 1997. In addition, two video cameras were deployed to collect continuous video data from 2-5 September 1997. The video data is used to infer surf zone information such as longshore current, breaker angle, and average wave period.					
<b>15. SUBJECT TERMS</b>  Surf zone, Oceanographic data, Validation, Refraction, Beach profile, Bathymetry					
<b>16. SECURITY CLASSIFICATION OF:</b>			<b>17. LIMITATION OF ABSTRACT</b>	<b>18. NUMBER OF PAGES</b>	<b>19a. NAME OF RESPONSIBLE PERSON</b>
<b>a. REPORT</b>	<b>b. ABSTRACT</b>	<b>c. THIS PAGE</b>	UL	29	Richard A. Allard
UNCLASSIFIED	UNCLASSIFIED	UNCLASSIFIED			<b>19b. TELEPHONE NUMBER (include area code)</b> (288) 688-4894

## CONTENTS

1. INTRODUCTION .....	1
2. OVERVIEW OF CAMP LEJEUNE MODELS .....	2
2.1 NORAPS .....	2
2.2 WAM .....	3
2.3 ADCIRC .....	3
2.4 STWAVE .....	4
2.5 REFDIF .....	4
2.6 SURF96 .....	4
3. INSTRUMENTATION .....	5
3.1 Sea-Bird Wave and Tide Recorder .....	5
3.2 XTG Wave and Tide Gauge .....	5
3.3 Deep-Water Measurements .....	6
3.4 Video Data .....	6
4. MODEL/DATA COMPARISONS .....	8
4.1 NORAPS Verification .....	8
4.2 WAM Verification .....	11
4.3 ADCIRC Verification .....	14
4.4 STWAVE Verification .....	17
4.5 REFDIF Verification .....	20
4.6 SURF96: Comparison with Video Data .....	22
5. SUMMARY AND CONCLUSIONS .....	24
6. ACKNOWLEDGMENTS .....	24
REFERENCES .....	25

# VALIDATING A COUPLED SUITE OF WAVE, TIDE, AND SURF MODELS AT ONSLOW BAY, NORTH CAROLINA

## 1. INTRODUCTION

In this study, a suite of “off-the-shelf” wave, tide, and surf models are coupled to produce a physically consistent dynamic representation of the surf zone for Onslow Beach, North Carolina. Many of the models used in this study have undergone some degree of validation, however, the suite of models has not been evaluated.

The Integrated Ocean Program (IOP) model suite consists of

- the deep-water wave model (WAM)
- two shallow-water wave refraction models
  - STWAVE (STeady state WAVE model)
  - REFDIF (REFraction/DIFraction model)
- the ADvanced CIRCulation (ADCIRC) model which predicts water elevations and depth-averaged currents
- an R&D version of the Navy Standard Surf Model (SURF96)

Atmospheric forcing for the models was provided by the Navy Operational Regional Atmospheric Prediction System (NORAPS). Figure 1 illustrates the IOP modeling strategy in which the regional WAM wave model is coupled to a series of shallow-water wave, tide, and surf models. Figure 2 depicts the model domain encompassing the region of interest for this study, the North Carolina coast.

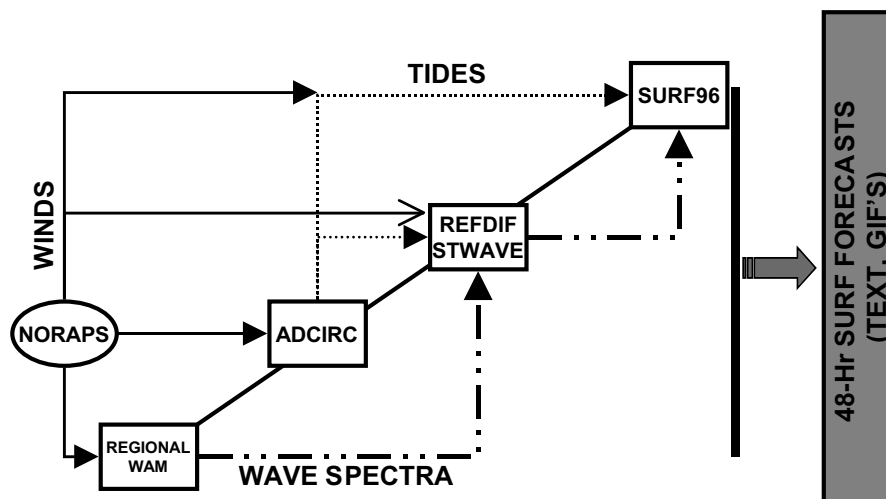
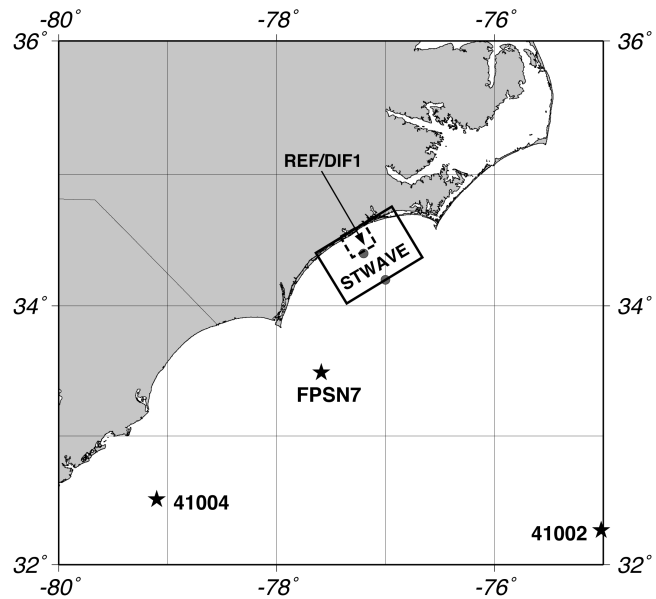


Fig. 1 – IOP modeling strategy

Fig. 2 – WAM domain for Carolina coastal area. Buoy locations (41002 and 41004) and C-MAN station FPSN7 are used for model comparison. The STWAVE and REF/DIF model areas are also shown. Circles denote locations of WAM directional spectra applied at shallow-water wave model outer boundaries.



To evaluate the IOP suite of models, a series of oceanographic instruments were deployed in shallow water at Onslow Beach to measure wave heights, wave periods, and tidal elevations. Wave and tide measurements were collected during the Joint Task Force Exercise (JTFEX 97-3) for the period 28 August – 5 September 1997. In addition, two video cameras were deployed to collect continuous video data from 2-5 September 1997. The video data are used to infer surf zone information such as longshore current, breaker angle, and average wave period.

The IOP modeling approach was developed to meet the requirements of the modeling and simulation community. However, IOP can address operational concerns as shown by recent demonstrations at JTFEX 97-2, Camp Pendleton, California; JTFEX 97-3, Camp Lejeune, North Carolina; and (NATO) exercise Strong Resolve in southern Spain in March 1998.

Section 2 presents an overview of the models used for this validation study. The instruments deployed near Onslow Beach are discussed in Section 3. Model/data comparisons are presented in Section 4. This report concludes with summary and conclusions in Section 5.

## 2. OVERVIEW OF CAMP LEJEUNE MODELS

This section gives a high-level overview of the models used in this validation study. Reference 1 provides a more complete description of the models set up specifically for Onslow Bay.

### 2.1 NORAPS

Wind and sea level pressure forcing used to drive the IOP model suite were provided by NORAPS, a mesoscale atmospheric model and data assimilation system [2] developed for and used by the U.S. Navy for many years. In 1998, the U.S. Navy started replacing NORAPS with an improved, higher-resolution Coupled Ocean Atmosphere Mesoscale Prediction System (COAMPS).

Continental United States (CONUS) NORAPS 10-m winds were used as inputs to WAM, ADCIRC, and STWAVE hindcasts for Onslow Bay. CONUS NORAPS has a horizontal resolution of  $0.5^\circ$  and was run twice daily, providing forecast products at 3-h intervals. NORAPS winds were accessed through the Master Environmental Library (<http://mel.dmsomil>) for the period 24 August – 5 September 1997.

## 2.2 WAM

The WAM wave model is a spectral wave prediction model developed by the WAMDI Group [3,4], an international consortium of wave modelers. WAM describes the sea surface as a discretized two-dimensional (2-D) spectrum of sea surface elevation variance density. The Fleet Numerical Meteorology and Oceanography Command (FNMOC) and Naval Oceanographic Office (NAVO) run operational global and regional implementations of WAM Cycle 4 [5]. WAM used in this study is the Carolina regional WAM (NC WAM) run by NAVO with a  $0.2^\circ$  resolution and spectra saved at selected locations. This regional WAM is coupled to the  $1^\circ$  north Atlantic WAM. This implementation of the regional WAM is not run routinely by NAVO. Rather, it is used for exercise support.

WAM is discretized into 25 frequency bands with center frequencies ranging from 0.04333 to 0.32832 Hz, with each frequency being 1.1 times that of the next lower band. Direction is discretized into 24 bands of width  $15^\circ$ . WAM computes the wind-generated energy density of each spectral component. Energy is also propagated in space, with refraction due to depth variation, and dispersion due to the nature of the waves. Because WAM spatial resolution does not resolve bathymetric variations close to a coast, WAM's refraction calculations apply to offshore regions rather than to the regions covered by STWAVE and REFDIF.

In this study, a 10-day period ranging from 24 August – 5 September 1997 was selected in which WAM wave spectra were saved and subsequently used as inputs to the STWAVE and REFDIF shallow-water wave models. Figure 2 shows the WAM domain and locations of the spectra used as inputs to STWAVE and REFDIF.

## 2.3 ADCIRC

The hydrodynamic model ADCIRC-2DDI [6-7] was selected to calculate water surface elevations and currents in the nearshore. The water elevations serve as input conditions for nearshore wave models. This 2-D, finite-element model uses tidal constituents, wind, and atmospheric pressure as input and outputs water surface elevations and currents. Reference 1 provides a more complete description the Camp Lejeune ADCIRC Modeling Procedures.

Figure 3 shows the ADCIRC grid for the North Carolina coast, including Camp Lejeune. The grid resolution is approximately 0.5 km near Camp Lejeune with higher resolution near the coastal inlets. Wind speed, wind direction, and sea level pressure used as input to ADCIRC were provided by the  $0.5^\circ$  resolution CONUS NORAPS (Section 2.1). M2 semidiurnal tidal constituents of amplitude and phase input along the grid boundary were supplied from the Dredging Research Program tidal constituent database [8].

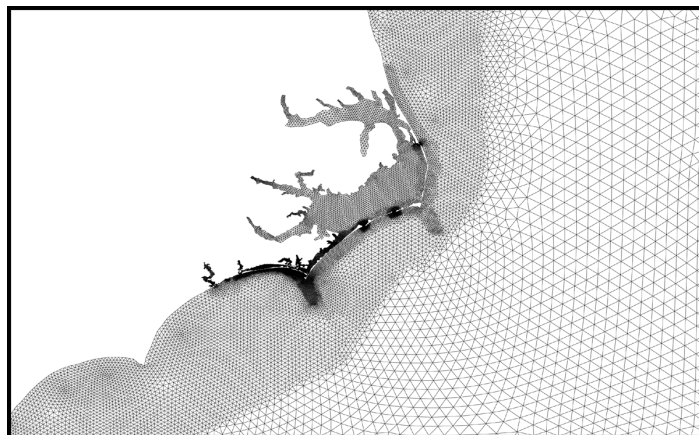


Fig. 3 – ADCIRC grid for Onslow Bay region

## 2.4 STWAVE

The spectral wave transformation model STWAVE [9-11] was implemented in this study to transform offshore wave spectra that were hindcast using the WAM model into nearshore and the surf zone. The circulation model ADCIRC [7] was used to calculate water surface elevation and used in the STWAVE hindcasts. Reference 1 provides a comprehensive description of the implementation of the Onslow Bay STWAVE model used in this study.

The STWAVE model used in this study had a horizontal resolution of 250 m and was forced on the outer boundary with WAM spectra at 33.0°N, 74°W. In addition, NORAPS wind speed and direction were specified along the outer boundary. Depth changes due to the wind and tide, calculated from ADCIRC, were included in these simulations. Bathymetry was provided by Naval Research Laboratory (NRL) at a 100-m resolution. STWAVE was run at 3-hr intervals for the period 24 August – 6 September 1997. Output saved at 3-h intervals includes: significant wave height, peak period, wave direction, and directional spectra. Figure 2 shows the STWAVE model domain.

## 2.5 REFDIF

The coastal wave model REFDIF [12] was implemented in this study to simulate waves in shallow water because of its rigorous treatment of combined refraction and diffraction processes. REFDIF is a monochromatic phase-resolving model that is well suited for areas with complex coastlines and offshore features such as islands. In this effort, a transfer function approach is used in which calculations are made for all possible frequency and angular components. The transfer function at any point in the model domain consists of an amplitude ratio and phase difference as a function of the input wave frequency and direction. For any given wave spectrum input, the spectrum is first divided into many wave components. The amplitude and direction of individual wave components is modified by the corresponding transfer function for a given location. The results from individual components are linearly combined to provide a final result. A transfer function approach, valid as long as local bathymetry does not change appreciably with time, can greatly reduce the processing time required produce refracted wave spectra. The transfer function results are not valid in the surf zone.

REFDIF was run for a series of hindcasts for Onslow Bay, for the period 24 August – 6 September 1997. Refraction and shoaling coefficients were created by running a series of REFDIF model simulations for a combination of 1278 wave directions and frequencies. The REFDIF model grid has a resolution of 92.5 m and was forced on the outer boundary with WAM spectra at the location 34.4°N, 77.2°W. A grid rotation of 30° (same rotation angle as STWAVE) was chosen so offshore depth contours were nearly parallel to the grid boundary. REFDIF directional spectra were saved at a series of locations for comparison with in situ data collected during this period. Reference 1 provides a more complete description of the implementation of REFDIF for Onslow Bay.

## 2.6 SURF96

SURF96 is a parametric one-dimensional (1-D) model based on the work of Thornton and Guza [13-14]. SURF96 is a random wave model for wave height transformations and longshore currents as waves cross the surf zone. It provides numerical and analytical solutions for cross-shore distributions of various parameters such as wave height, longshore current velocity, and wavelength. SURF96 is a research version of SURF3.0, a major upgrade to the Navy Standard Surf Model (NSSM), which was delivered to the Oceanographic and Atmospheric Model Library (OAML) in February 1999. Reference 15 provides a more complete description of SURF3.0.

The model is designed to operate in a variety of modes to provide both military and civilian users with local surf and current forecasts. SURF96 requires four inputs to perform calculations: (1) depth profile, (2) directional wave spectrum, (3) water level, and (4) wind direction and wind speed. SURF96 hindcasts were performed for Onslow Beach, using directional wave spectra from two refraction models: (1) STWAVE and (2) REFDIF. The beach profile used in this study, shown in Fig. 4, was based on data from a Navy SEAL survey collected during the Purple Star exercise in April 1996 [16]. Water level information was provided by the ADCIRC hindcast model runs. Observed hourly winds were provided by the U.S. Marine Corps Air Station at Camp Lejeune.

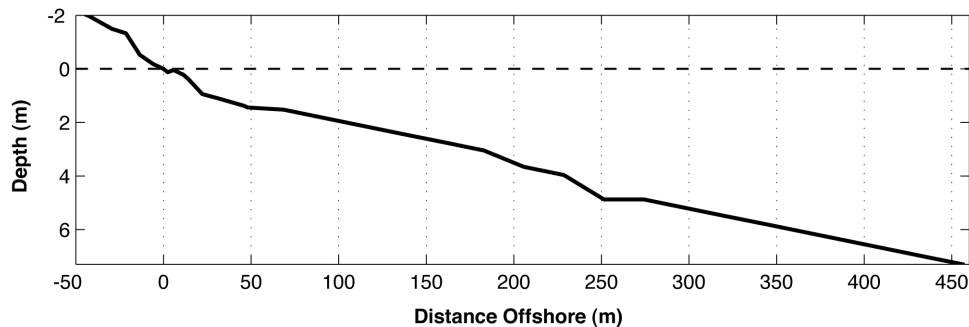


Fig. 4 – Beach profile used for surf model hindcasts at Onslow Beach

### 3. INSTRUMENTATION

This section describes data recorded and archived by a network of meteorology and oceanography (METOC) sensors that were deployed in very shallow water and surf zone environments from 26 August – 6 September 1997. Key meteorological parameters included wind speed, wind direction, air temperature, and pressure. Two weather stations were deployed from Camp Lejeune’s Risley Pier. Traditional cup and vane anemometers were used to measure wind speed and direction. Oceanographic instruments included five Sea-Bird Seagauge wave and tide recorders (SBE26), four prototype expendable tide gauges (XTG), and a video data collection system operated by NRL’s Marine Geosciences Division.

#### 3.1 Sea-Bird Wave and Tide Recorder

Five Sea-Bird Seagauge wave and tide recorders (SBE26) were deployed in Onslow Bay, during the period 26 August – 5 September 1997 at depths ranging from 1 to 10 m of water. The SBE26 uses a precision pressure, thermometer, and conductivity sensor to provide high-resolution water level, wave, and temperature data. Figure 5 shows the locations of the SBE26 instruments. Software provided by the manufacturer was used to process the wave and tide gauge data.

#### 3.2 XTG Wave and Tide Gauge

A portable, low-cost tide gauge developed for the U.S. Navy was deployed at four locations in Onslow Bay. The XTG uses a low-cost pressure sensor and thermistor to provide low-frequency water levels and nondirectional wave information. One of the instruments, XTG-004, reported inconsistent significant wave height readings. This pressure offset was traced back to a failed solder joint on the printed circuit board. XTG-004 data were not used in subsequent analyses. The remaining XTGs dropped a record approximately every 16 h. These outliers were caused when data were being written to flash memory. Linear interpolation between endpoints was used to smooth these drops in the data. Figure 5 shows the XTG locations.

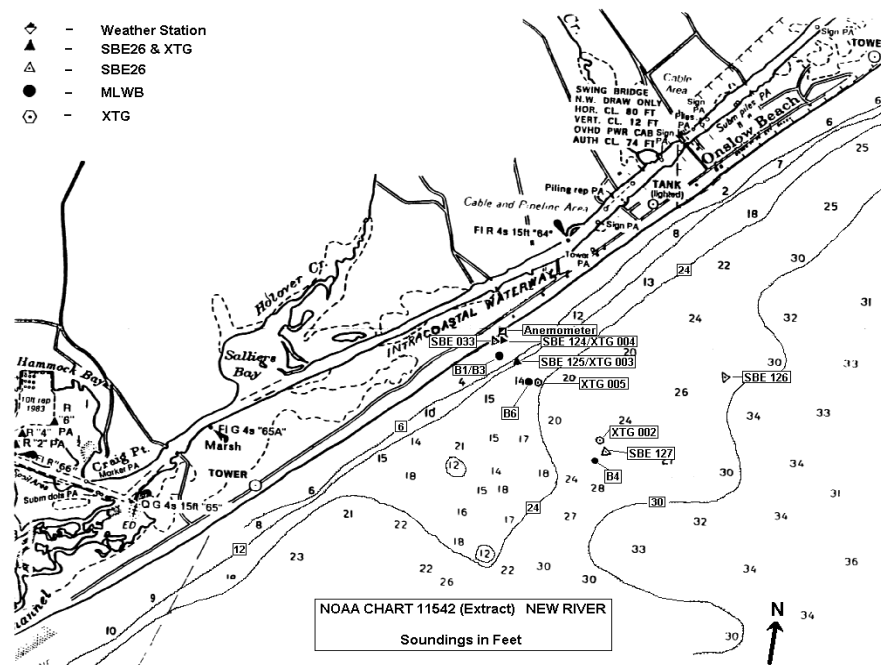


Fig. 5 – Instrumentation network. Deployment locations along Onslow Beach during JTFEX 97-3.

### 3.3 Deep-Water Wave Measurements

The National Oceanic and Atmospheric Administration's (NOAA) National Data Buoy Center (NDBC) has an instrument platform network consisting of approximately 70 moored buoys, 58 Coastal-Marine Automated Network (C-MAN) sites, and 14 Profiler Surface Observing System sites. The types are 3-, 10-, or 12-m discuss hulls, 6-m boat-shaped Naval Oceanographic and Meteorological Automated Device (NOMAD) hulls, and Coastal Oceanographic Line-of-Sight buoys. NDBC's moored buoys measure and transmit barometric pressure, wind direction and speed, air and sea temperature, wave direction and wave energy spectra from which significant wave height, dominant wave period, and average wave period are derived.

Outside of Onslow Bay, there are three NDBC stations (i.e., 41002, 41004, and FPSN7). Station 41002 consists of a NOMAD buoy moored approximately 149 nm southeast of Onslow Beach at a depth of 3,785.6 m. Station 41004 consists of a 3-m discus buoy moored in 38.4 m of water and approximately 55 nm southeast of Charleston, South Carolina. Station FPSN7 is the Frying Pan Shoals C-MAN station. Figure 2 shows the locations of all three buoys. The anemometer at C-MAN FPSN7 is located at a height of 44 m. A power law relationship was used to reduce the wind speed to a 10-m height, consistent with the NORAPS winds. Wind measurements on buoys 41002 and 41004, located at a height of 5 m, were not adjusted.

### 3.4 Video Data

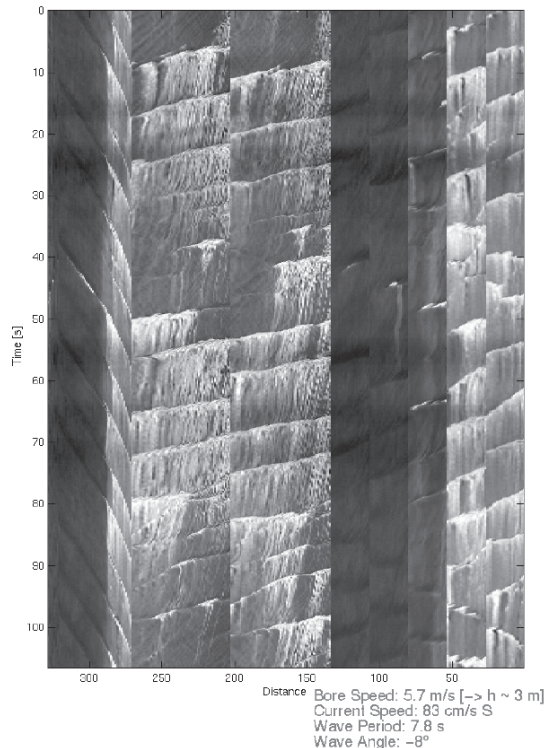
Surf zone environmental processes were estimated using video imaging processing techniques [17] that allowed quantification of hydrodynamical and geological parameters including wave period, wave angle, wave speed, surf zone width, longshore current, shoreline location, and sandbar structure. Two video cameras were installed at Onslow Beach, during JTFEX 97-3. One camera was mounted atop the roof of a small building on Risley Pier; the other camera (looking north) was mounted in a tower approximately 400 m south of Risley Pier.

Figure 6 shows a virtual instrument array in the cross-shore and alongshore direction. Pixel intensity time series sampled at each of the dotted locations allowed hydrodynamic properties to be computed, e.g., computation of hydrodynamic properties. Figure 7 shows an example time series for eight arrays. The first column of imagery clearly represents the onshore progression of waves (left to right) from which an average wave period and speed can be determined.



Fig. 6 – Virtual instrument array which allows quantification of nearshore oceanographic parameters. Analysis of pixel intensity time series sampled at each of the dotted locations allows hydrodynamic properties such as wave period, incidence angle, and alongshore currents to be computed.

Fig. 7 – Example of pixel intensity data from eight virtual arrays at Onslow Beach. The first column of imagery represents pixels sampled along a cross-shore line such that waves move from offshore to onshore (left to right) with time increasing down on the page. The next several columns show alongshore array results that indicate a wave period of 8 s and a longshore current of ~83 cm/s to the south.



#### 4. MODEL/DATA COMPARISONS

This section evaluates each component of the IOP model suite: WAM, STWAVE, REFDIF, ADCIRC, and SURF96. Comparisons are made against available data. Although NORAPS (and subsequently COAMPS) is not part of IOP, the wind forcing is evaluated since it is used to drive many of the models in this study.

##### 4.1 NORAPS Verification

CONUS NORAPS 10-m winds were used to force the NC WAM, ADCIRC, and STWAVE hindcasts during the period 24 August – 5 September 1997. Table 1 presents summary statistics between the three NDBC buoys (shown in Fig 2) and NORAPS winds interpolated to each buoy location. Figures 8 and 9 show comparison plots of buoy observations and NORAPS wind speed and direction.

Offshore weather conditions during the period 28 August – 5 September were marked by two significant meteorological events depicted in Fig. 10. A low-pressure system located near 32°N, 77°W at 0000 Z on

Table 1 – NORAPS Error Statistics

<b>NORAPS Error Statistics (Wind Speed)</b>					
Buoy	Mean Error (m/s)	Mean Error (%)	Mean RMS Error (m/s)	Mean RMS Error (%)	Correlation Coefficient
41002	-0.05	-0.9	0.2	2.3	0.53
41004	-1.10	-17.8	-1.1	-16.0	0.73
FPSN7	0.35	5.0	0.6	7.6	0.66
<b>NORAPS Error Statistics (Wind Direction)</b>					
Buoy	Mean Error (deg)	Mean Error (%)	Mean RMS Error (deg)	Mean RMS Error (%)	Correlation Coefficient
41002	-13.6	-112.0	-13.5	9.3	0.58
41004	-11.7	-13.5	-10.1	8.5	0.88
FPSN7	-9.3	-11.5	-9.7	-8.6	0.62
<b>NORAPS Error Statistics (Sea Level Pressure)</b>					
Buoy	Mean Error (mb)	Mean Error (%)	Mean RMS Error (mb)	Mean RMS Error (%)	Correlation Coefficient
41002	0.09	0.01	0.09	0.01	0.95
41004	0.62	0.06	0.62	0.06	0.79
FPSN7	-0.76	-0.08	-0.76	-0.08	0.99

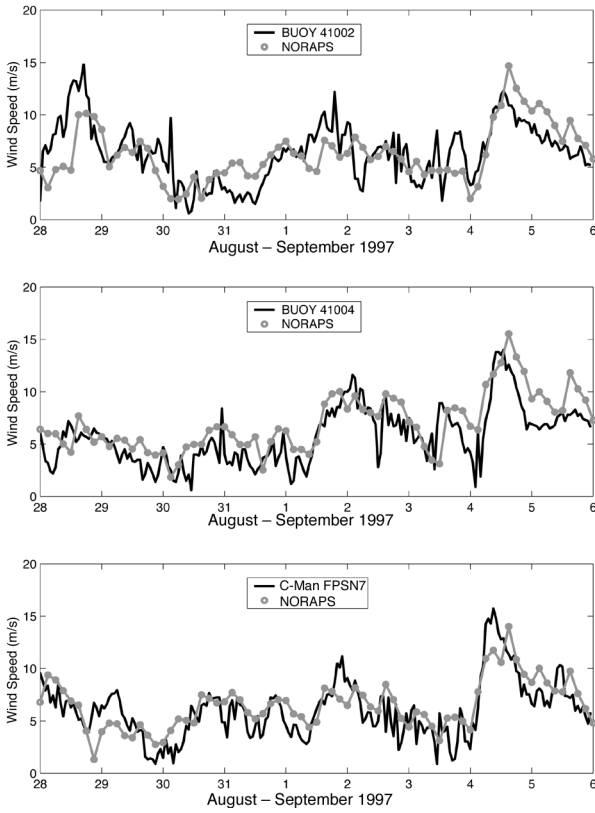


Fig. 9 – Comparison between NORAPS wind direction and NDBC buoys

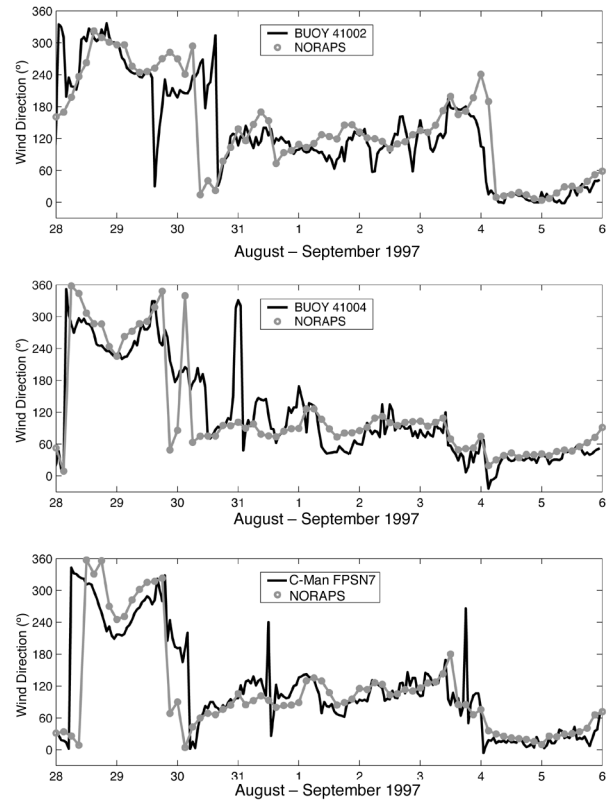


Fig. 8 – Comparison between NORAPS wind speed and NDBC buoys

28 August moved through the western Atlantic coastal waters causing high seas as observed at buoy 41002. Another low-pressure system and trailing cold front near 30.5°N, 79°W at 1200 Z on 3 September intensified and moved east. Wave heights at all three buoys increased to 3-4 m on 4 September. Further discussions on wave conditions continue in Section 4.2.

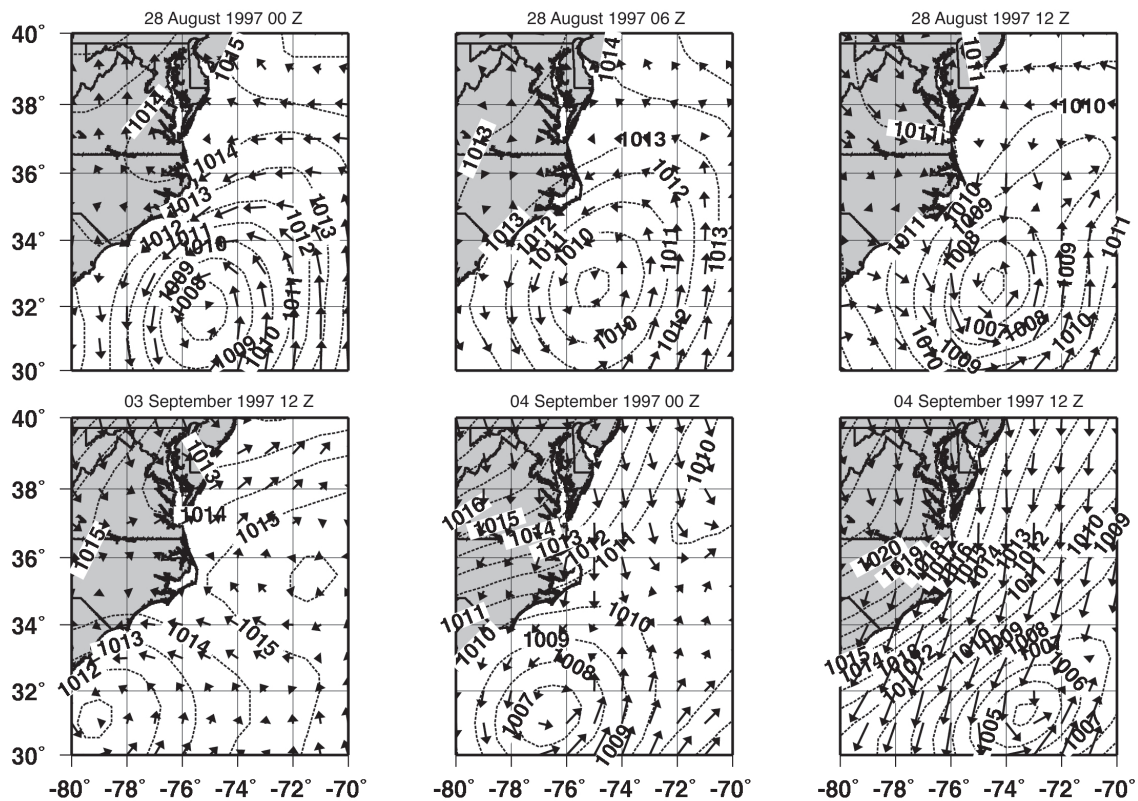


Fig. 10 – NORAPS winds and sea level pressure (mb) for: 28 August 1997 at (a) 0000 GMT, (b) 0600 GMT, (c) 1200 GMT; 3 September at (d) 1200 GMT; and 4 September at (e) 0000 GMT and (f) 1200 GMT

The NORAPS model assimilates buoy information into its analysis; however, errors will increase as the forecast period increases. In this study, analyses were available every 12 h. Forecast winds and pressure fields were available at tau = 3, 6, and 9 h. Errors in NORAPS wind fields will translate into other models such as WAM and, subsequently, STWAVE.

#### *NORAPS Wind Speed*

The magnitude of the 10-m wind showed some variability between each platform. NORAPS wind speed at the location of buoy 41004 had the highest mean error at  $-1.1$  m/s while 41002 had the lowest mean error at  $-0.05$  m/s. Negative values of mean error indicate that the magnitude of the NORAPS winds was overpredicted. Correlations at all three buoys ranged from  $r = 0.53$  at buoy 41002 to  $r = 0.73$  at buoy 41004. Section 4.2 discusses how overprediction and underprediction of wind speed can affect the generation of waves in the deep-water WAM wave model. A possible explanation for the wind speed correlation values is that the measured buoy data exhibit greater variability than the  $0.5^\circ$  NORAPS atmospheric model.

*NORAPS Wind Direction*

Average mean error in NORAPS wind direction for all three buoys ranged from 9.3 to 13.6°. Some of this error can be attributed to the delay in NORAPS bringing cold fronts through the region, resulting in wind direction differences as high as 90° for durations up to 12 h. NORAPS wind directions showed higher correlations than wind speed, with buoy 41004 having the highest correlation at 0.88.

*NORAPS Sea Level Pressure*

NORAPS sea level pressure (not shown), applied in the ADCIRC model, showed very high correlations with values ranging from 0.79 at buoy 41004 to 0.99 at C-MAN station FPSN7 at Frying Pan Shoals.

**4.2 WAM Verification**

The regional NC WAM model was used in this study to provide directional wave spectra to the shallow-water wave refraction models STWAVE and REFDIF. Errors in NC WAM are passed along to these models. This section discusses the performance of NC WAM in comparison to three NDBC buoys contained within the NC WAM domain. Figures 11 and 12 compare observed and WAM significant wave height and mean wave period, respectively. Table 2 shows WAM error statistics for these parameters.

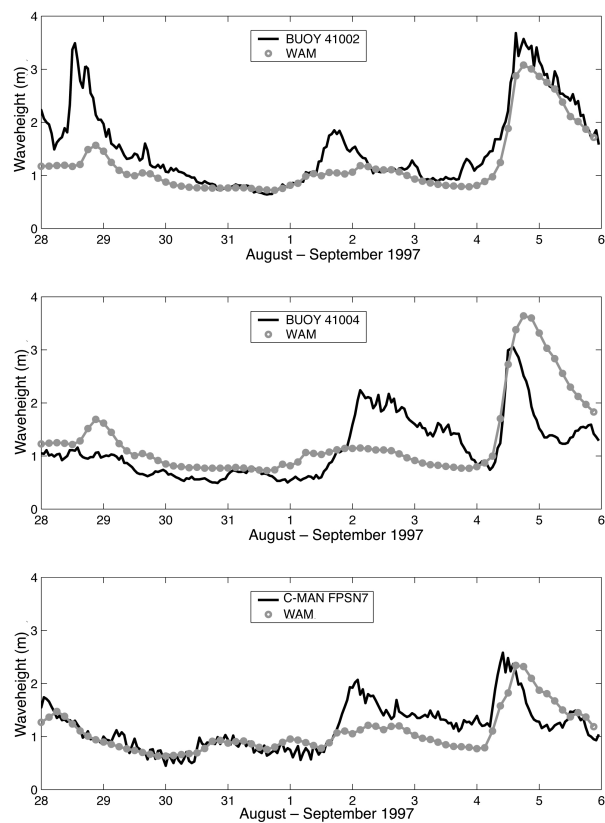


Fig. 11 – Comparison of WAM vs observed (buoy) wave heights

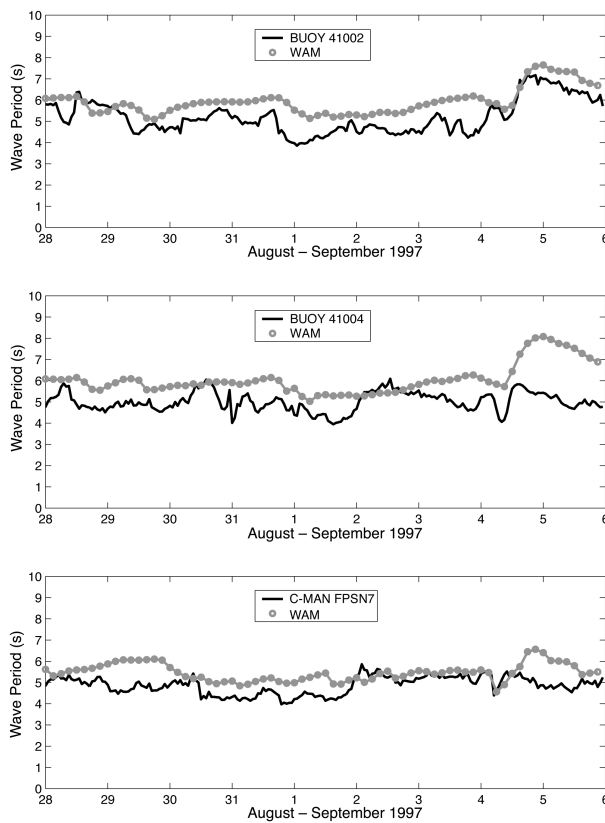


Fig. 12 – Comparison of average wave period from WAM vs buoy observation

Table 2 – WAM Error Statistics

WAM Error Statistics (Significant Wave Height)					
Buoy	Mean Error (cm)	Mean Error (%)	Mean RMS Error (cm)	Mean RMS Error (%)	Correlation Coefficient
41002	28	18.8	32	19.8	0.82
41004	-16	-13.5	-21	16.2	0.59
FPSN7	10	8.8	12	9.4	0.70
WAM Error Statistics (Mean Wave Period)					
Buoy	Mean Error (s)	Mean Error (%)	Mean RMS Error (s)	Mean RMS Error (%)	Correlation Coefficient
41002	-0.7	-13.4	-0.7	-13.0	0.73
41004	-1.1	-23.2	-1.1	-23.4	0.30
FPSN7	-0.60	-12.6	-0.6	-12.6	0.35

### Wave Heights

WAM significant wave heights compared favorably with buoy observations during this study. At buoy 41002, located near the southeast corner of the NC WAM boundary, the mean error was 28 cm with a correlation coefficient of 0.82. Two major wind-driven events occurred during this period. The first event, depicted in Figs. 10(a)-(c), shows a 1008-mb low pressure center near 32°N, 75°W, very close to buoy 41002 at 0000 GMT on 28 August. NC WAM underpredicts the observed wave height on this date by 2 m. An examination of NORAPS wind direction (see Fig. 9) on 28 August shows reasonable agreement with observed wind direction; however, NORAPS wind speeds were underestimated by as much as 50%. This discrepancy between modeled vs observed wind speed could account for much of the wave height difference. A minor episode on 1 September showed a 1-m increase in wave height at buoy 41002, while WAM indicated little change. NORAPS wind directions were 30° out of phase with observations and wind speeds were underestimated by 3 to 4 m/s, accounting for WAM “missing” this increase in wave height. The second event occurred on 4-5 September as a low-pressure system tracked off the Georgia coastal waters and headed east. A trailing cold front ushered in strong northerly winds to the entire area by 5 September. Figure 11 shows that WAM performed well at this location.

WAM wave heights at buoy 41004 show a mean error of -16 cm (13.5%) with a correlation coefficient of 0.59. Wave heights shown in Fig. 11 were reasonable from 28 August – 2 September; however, wave heights were underpredicted from 2-4 September. NORAPS wind speeds agreed well with buoy observations during this period, but NORAPS wind directions were about 30° out of phase, producing a wind with a more southerly component. The storm event on 4 September is modeled quite well from 0000 to 1200 GMT, but WAM overpredicts the wave height afterwards. NORAPS wind speeds are higher than observed at this time by 2 to 3 m/s accounting for this difference.

At C-MAN station FPSN7, wave heights compared very well during the period 28 August – 1 September. Similar to comparisons at buoy 41004, wave heights were underpredicted during 2-4 September. Overall, FPSN7 compared fairly well with observation, as indicated by a correlation coefficient of 0.70. Measurement errors for wave buoys typically are on the order of 10%. WAM had mean error in wave height of

8.8% at the location of the buoy at FPSN7, well within the range of instrument error. Because this is the closest observation station to the STWAVE and REFDIF modeling area, reasonable results were expected for the shallow-water wave models.

### Wave Periods

Table 2 presents WAM mean wave period error statistics. All three locations show mean wave period errors on the order of 1 s or less, which is within the range of the instrument accuracy of 1 s. Correlations were reasonable at 41002 ( $r = 0.73$ ) but were low at 41004 and FPSN7 with values of  $r = 0.30$  and  $r = 0.35$ , respectively. WAM periods were consistently higher than observation. This could be attributed to the method in which means were computed. WAM computes the mean period based on the mean of spectral components at each model output timestep (e.g., every 3 h). The NDBC computes the average wave period of all waves in a 20-min period, which could yield lower wave periods. Figure 12 shows a time series comparison of average wave period at all three buoy locations.

Figure 13 presents a summary depiction of observed winds, NORAPS winds, and WAM wave directions at each of the three buoy locations. There is a general agreement between the prevailing wind direction and wave direction. The strong cold frontal passage is evident at all locations near 0000 GMT on 4 September.

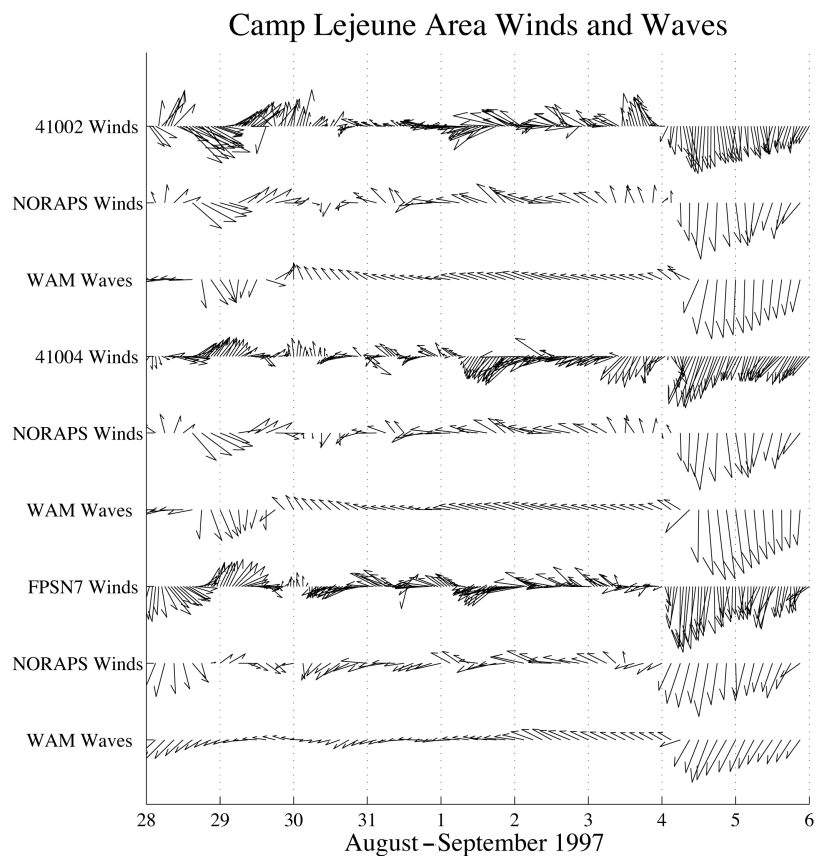


Fig. 13 – Time series of buoy wind direction and magnitude, NORAPS wind direction and magnitude, and direction in which WAM waves are moving toward. Vectors point in direction of motion.

### 4.3 ADCIRC Verification

ADCIRC water surface elevations are compared with Sea-Bird and expendable tide gauges at the four locations given in Table 3. The pressure measurements were converted to tide elevations by subtracting the mean pressure of the record and converting pressure to elevation with a constant factor of 0.6857 m/psi (changes in density with temperature were neglected). Figures 14 through 17 give time history plots of the tide for gauge pairings; Table 4 summarizes error statistics.

Table 3 – ADCIRC Verification Locations

ADCIRC Verification Location							
Sea-Bird Gauge	Latitude (°N)	Longitude (°W)	Expendable Tide Gauge	Latitude (°N)	Longitude (°W)	Gauge Depth (m)	ADCIRC point
SB0127	34°33'1.66"	77°16'39.06"	XTG002	34°33'3.77"	77°16'40.27"	9.1	19
			XTG005	34°33'15.95"	77°16'58.41"	7.6	17
SB0125	34°33'20.05"	77°17'4.95"	XTG003	34°33'20.05"	77°17'4.95"	3.0	18
SB0124	34°33'30"	77°17'10"	XTG004	34°33'30"	77°17'10"	2.1	18

Table 4 – ADCIRC Error Statistics

ADCIRC Error Statistics							
Sea-Bird Gauge	Mean Error (cm)	RMS Error (cm)	Correlation Coefficient	Expendable Tide Gauge	Mean Error (cm)	RMS Error (cm)	Correlation Coefficient
SB0127	1.9	.30	.92	XTG002	2.0	16.3	.92
				XTG005	2.0	15.8	.92
SB0125	1.9	.31	.91	XTG003	2.0	17.5	.91
SB0124	2.1	.31	.92	XTG004	4.8	18.9	.91

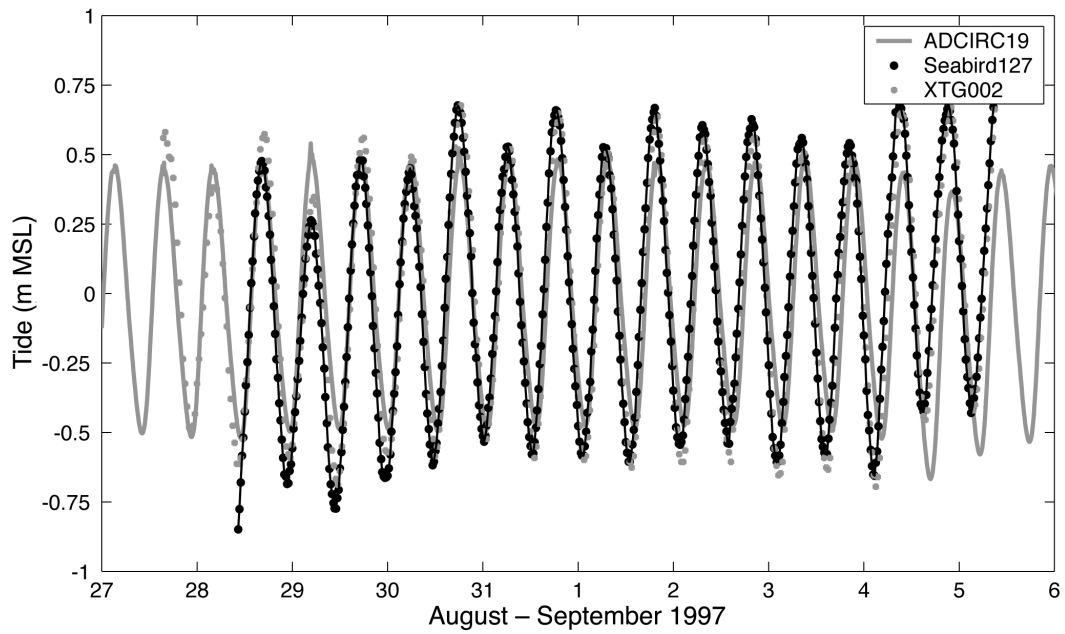


Figure 14 – ADCIRC tide comparison to SB0127 and XTG002

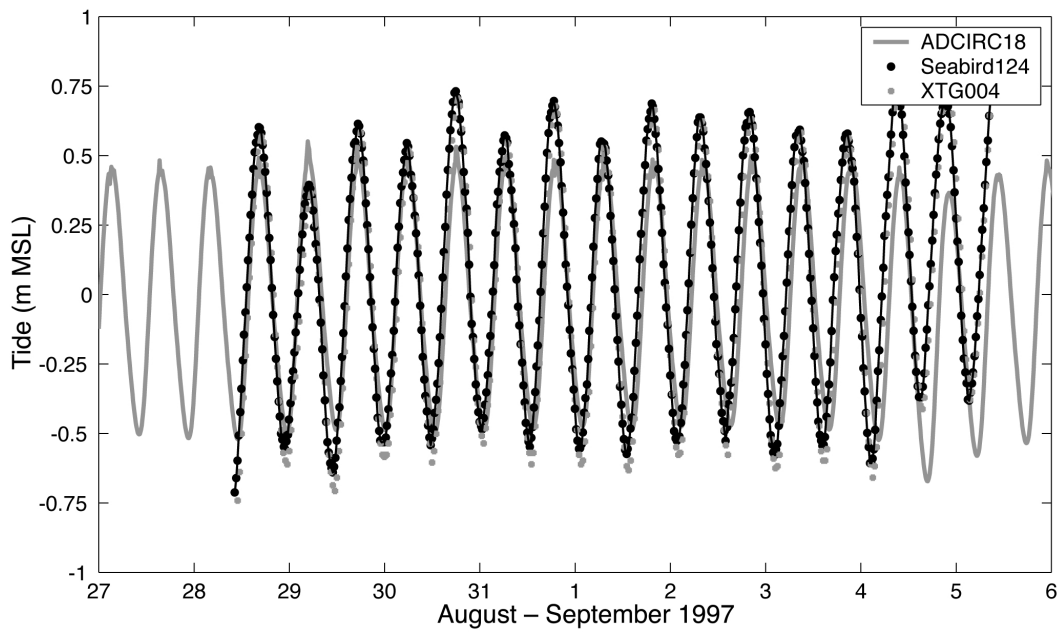


Fig. 15 – ADCIRC tide comparison to SB0124 and XTG004

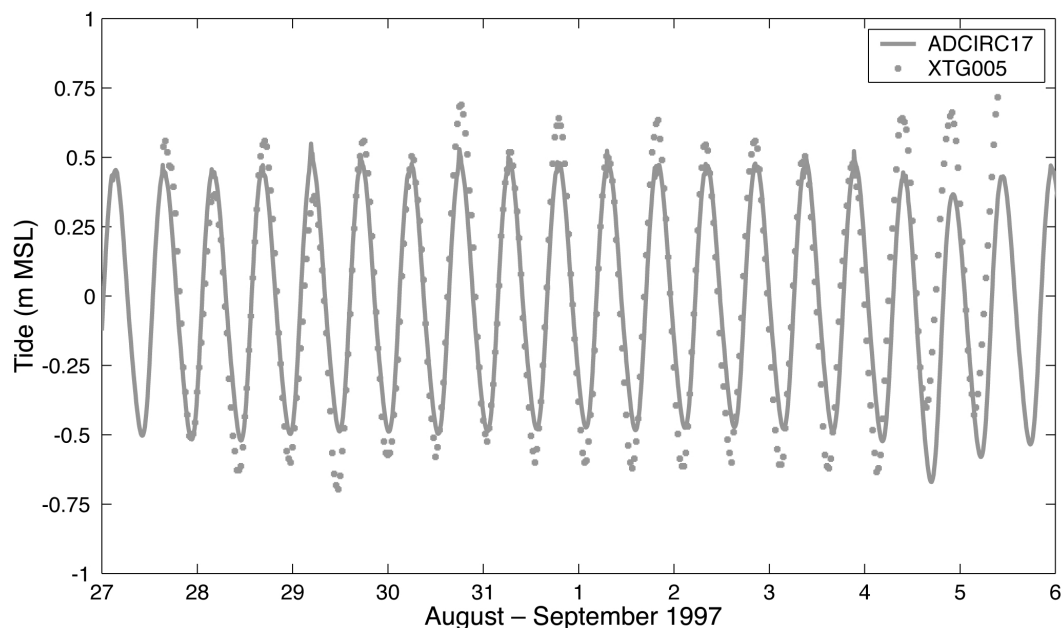


Fig. 16 – ADCIRC tide comparison to XTG005

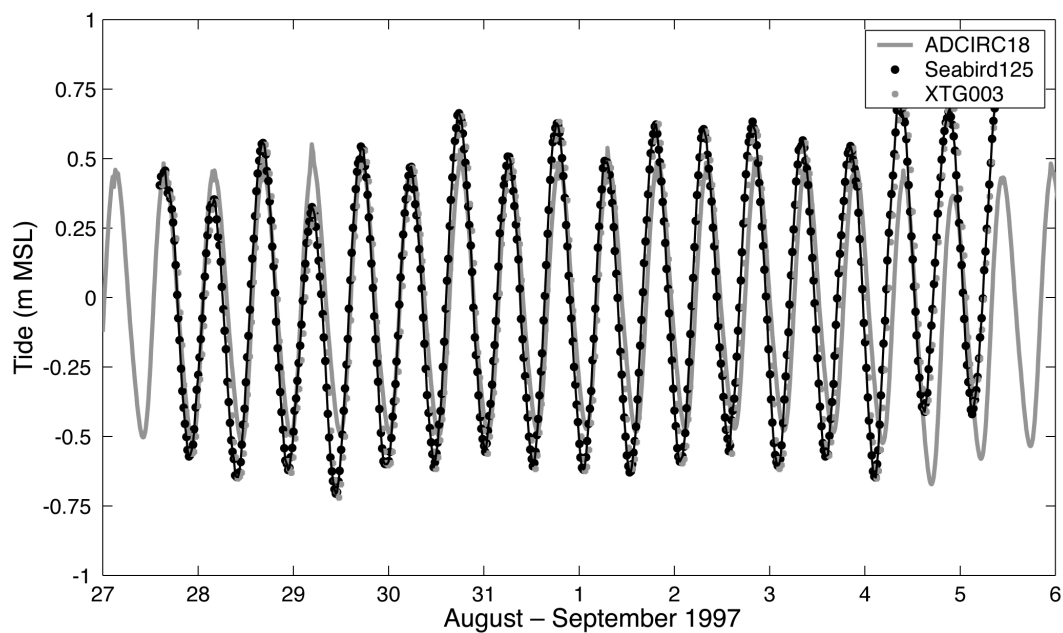


Fig. 17 – ADCIRC tide comparison to SB0125 and XTG003

The plots and error statistics show reasonable agreement between the ADCIRC predicted and measured tides. The tidal phasing agrees well, but the tidal amplitude is underpredicted by about 14%. Only the  $M_2$  tide was simulated with ADCIRC, which accounts for some of the underprediction and the lack of semidiurnal variation. One surprising difference between the measured and predicted tide is the measured mean tidal setup on 4 September. ADCIRC predicts a mean set down during this period due to the local winds. This difference is due to accuracy and resolution in the wind fields. The resolution of the ADCIRC grid in the nearshore is relatively coarse (0.5 km). The lack of resolution does not appear to greatly impact

the results for the tidal simulation but would be more important for storm events with strong winds and complex wind fields. The tidal amplitude increases in shallower depths (increase of about 5 cm between depth of 9 m and 2 m in the measurements), so better resolution of the bathymetry in ADCIRC would also improve nearshore amplitude estimates. The greatest improvement in results could be gained by adding additional tidal components to force ADCIRC.

#### 4.4 STWAVE Verification

To simulate nearshore wave transformation at Camp Lejeune, an STWAVE grid was generated with a 250-m resolution that extended 201 cells (50 km) in the cross-shore direction and 301 cells (75 km) in the longshore direction. STWAVE was driven with spectra calculated from a regional-scale NC WAM simulation. Nearshore winds input to the STWAVE simulations were generated by NORAPS. WAM spectra and NORAPS winds were extracted at 3-h intervals at the location 34.2°N, 77°W for input to STWAVE. Tide elevations input to STWAVE were from the ADCIRC simulation.

STWAVE output is compared with Sea-Bird wave measurements at the four locations given in Table 5. Note that the gauge and model depths differ by 10 to 70%. The inner gauges are in very shallow depths that are not well-resolved with the 250-m STWAVE grid spacing. Figures 18 through 20 are time history plots of wave height and period for each of the model-gauge pairings. Figures 18(a) through 20(a) present significant wave height (defined as the zero-moment wave height), and Figs. 18(b) through 20(b) present average wave period. Gauges SB0124 and SB0033 are given on the same plot because they both map into the same STWAVE grid cell. Table 6 summarizes error statistics.

Table 5 – STWAV Verification Locations

STWAVE Verification Locations					
Gauge	Latitude (°N)	Longitude (°W)	Gauge Depth (m)	STWAVE Grid Point	STWAVE Depth (m)
SB0127	34°33'1.66"	77°16'39.06"	9.1	(187, 154)	8.2
SB0125	34°33'20.05"	77°17'4.95"	3.0	(190, 155)	5.0
SB0124	34°33'33"	77°17'10"	2.1	(191, 155)	2.6
SB0033	34°33'27.68"	77°17'11.78"	1.5	(191, 155)	2.6

Table 6 – STWAVE Error Statistics

STWAVE Error Statistics								
Location	Waveheight					Wave Period		
	Mean Error (cm)	Mean Error (%)	RMS Error (cm)	RMS Error (%)	Correlation Coefficient	Mean Error (s)	RMS Error (s)	Correlation Coefficient
SB0127	3.5	7.1	19.1	31.8	0.75	-.4	0.8	0.32
SB0125	3.9	7.8	18.1	33.0	0.72	.1	0.7	0.55
SB0124	7.0	12.8	16.9	30.1	0.76	.1	0.9	0.42
SB0033	2.9	3.5	18.1	40.3	0.51	.2	0.6	0.70

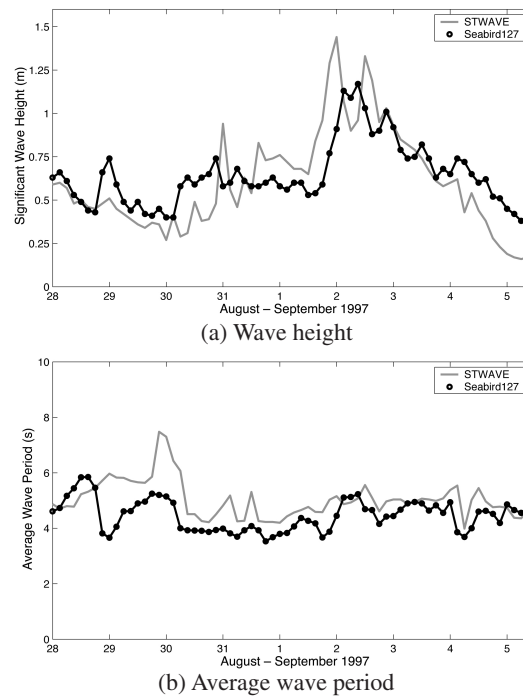


Fig. 18 – STWAVE comparison to SB0127

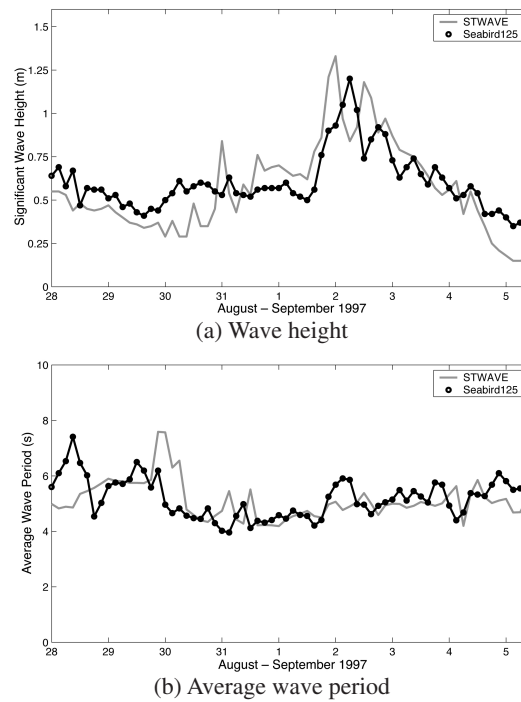


Fig. 19 – STWAVE comparison to SB0125

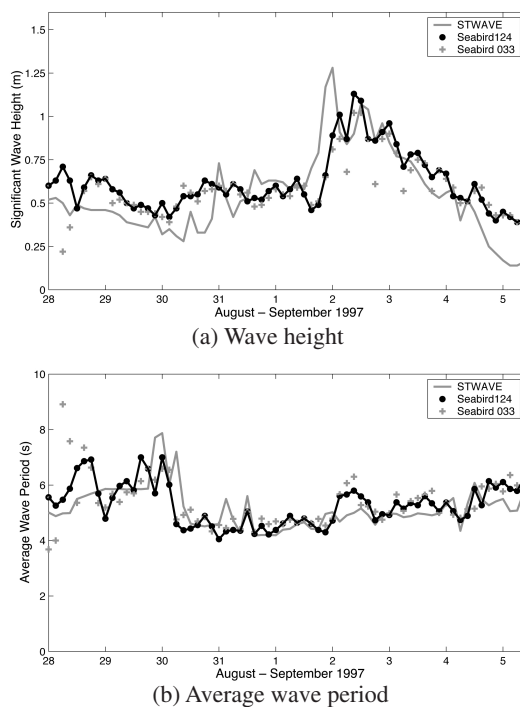


Fig. 20 – STWAVE average wave period comparison to SB0124 and SB033

### Wave Height

The average mean error in wave height is 7.8% and the average root-mean-square (RMS) error is 34%. The positive mean error indicates that STWAVE underpredicts the gauge measurement. Measurement errors for pressure gauges are typically on the order of 10%. In general, the STWAVE heights follow the trend of the measurements. Two features in the time histories show up at each gauge: STWAVE overestimates wave height early on 2 September and underestimates wave height around 5 September. These features are consistent with WAM (STWAVE input) comparisons to deep-water buoys. The correlation coefficients between gauge data and model results average 0.74 (neglecting gauge SB0033), which is in the range of correlations between WAM and buoy measurements (0.59 to 0.82). The largest RMS errors occur at the shallowest gauge (SB0033). The greater errors at this gauge occur during 2-3 September, when wave heights are larger and waves are breaking at low tide at the gauge (note the 12-h oscillation in wave height at SB0033). The 1.1-m depth difference between the gauge and the model comparison point (see Table 5) can potentially cause differences in wave height up to 0.7 m in the surf zone (height-to-depth ratio of 0.64 times the depth difference of 1.1 m). Improved model results could be obtained by increasing the STWAVE grid resolution (STWAVE resolution was selected to provide accurate forcing to drive the Navy Standard Surf Model and not to resolve the surf zone) and improving the STWAVE input spectra (more accurate WAM simulation or offshore gauge data).

### Wave Period

To compare the measured and modeled wave periods, the average wave periods were calculated from the spectra,

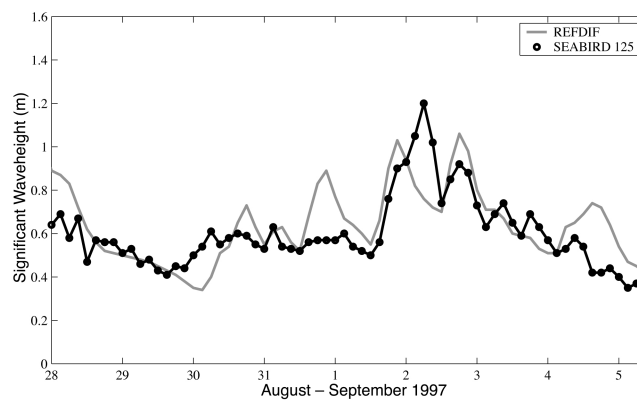
$$T_{average} = \frac{\sum E(f)\Delta f}{\sum fE(f)\Delta f}, \quad (1)$$

where  $E(f)$  is the spectral energy density at frequency  $f$  and  $\Delta f$  is the frequency increment. The average mean error in wave period is 0.2 s and the average RMS error is 0.7 s. Accuracy of wave period measurements is on the order of 1 s. The plots of average wave period show that differences between the measured and calculated periods are generally less than 1 s, but the variation in the average wave period is also small (less than 0.4 s). The correlation coefficients range from 0.3 to 0.7. The relatively low correlations reflect the fact that average periods are fairly constant and the variability is on the order of the measurement accuracy of 1 s.

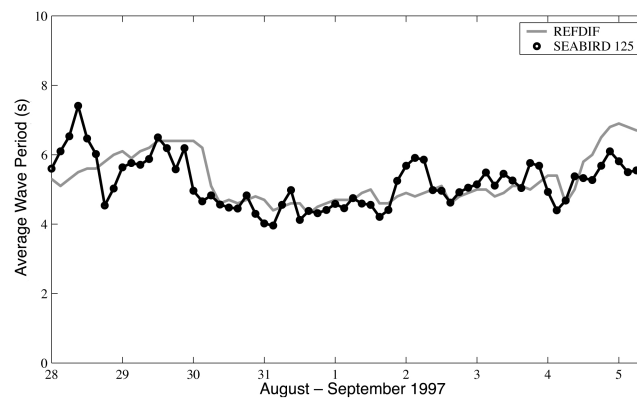
#### 4.5 REFDIF Verification

Four wave gauges were available for comparison. However, the REFDIF transfer function approach is only applicable at depths where waves are not breaking. Consequently, SB0124 and SB033, located at depths of 2.1 and 1.5 m water depth, respectively, were too shallow to be used in this study. SB0127 at a depth of 9.1 m was considered too close to the model boundary (18 m) to have significant wave transformation. Therefore, only SB0125 was used for comparison. The corresponding REFDIF grid point (185,122) is at a depth of 6 m. The tidal range was less than 1 m in the modeling area (i.e., maximum 0.5-m adjustment to the depth grid ranging from 18 to 6 m) which does not significantly modify the transfer function. Therefore, no tidal adjustment to depth was applied.

Figure 21 shows the comparison of significant wave height and average wave period between REFDIF and SB0125. In general, the model results agree with the gauge data. Table 7 summarizes error statistics.



(a) Significant wave height



(b) Average wave period

Fig. 21 – REFDIF comparison to SB0125

Table 7 – REFDIF Error Statistics at SB0125

<b>Significant Waveheight Error Statistics at SB0125</b>				
Mean Error (cm)	Mean Error (%)	RMS Error (cm)	RMS Error (%)	Correlation Coefficient
4	8.4	16	25.8	0.55
<b>Average Period Error Statistics at SB0125</b>				
Mean Error (s)	Mean Error (%)	RMS Error (s)	RMS Error (%)	Correlation Coefficient
0.1	3.0	0.6	11.6	0.62

### Wave Height

REFDIF in general follows the trend of SB0125. Between 31 August and 3 September, REFDIF shows more variability than SB0125. This is attributed to the WAM directional input, which shows more peaks during this period. In general, SB0125 shows fluctuations that can be attributed to local wind wave generation. The WAM input data from REFDIF is updated every 3 h whereas the SB0125 continuously measures the local waves at a sampling rate of 1 Hz. The correlation coefficient of 0.55 is lower than that for STWAVE, which had a value of 0.72. The model has a mean error of 8.4% or 4 cm. These moderately low values reflect that the scatter is almost evenly distributed along the dashed line as shown in Fig. 22. In view of that WAM input can introduce error into REFDIF, the prediction is quite acceptable.

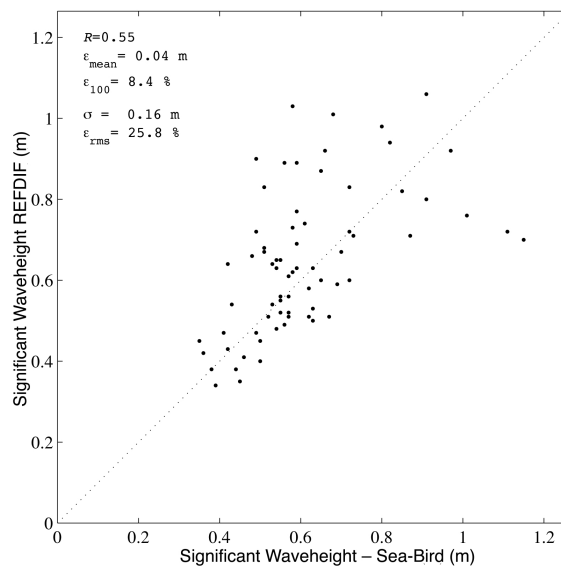


Fig. 22 – Scatter plot of significant wave height between REFDIF and SB0125

### Wave Period

The same definition of average wave period as STWAVE is used in this discussion. As shown in Fig. 21(b), REFDIF results follow SB0125 quite well, except that the model shows higher wave periods near 5 September. This deviation can be attributed to WAM input data as discussed earlier. The mean error is 3% and 0.1 s; in this instance, REFDIF gives slightly better average period prediction than STWAVE. However, STWAVE compared results at four locations; REFDIF is only evaluated at one location.

#### 4.6 SURF96: Comparison with Video Data

SURF96 hindcasts were performed with two shallow-water wave models as inputs: STWAVE and REFDIF. For both sets of hindcasts, the same water level information, beach profile, and wind inputs were used. The only difference was that the nearshore directional wave spectra was used as SURF96 input.

Table 8 presents a comparison between SURF96 output based on REFDIF and STWAVE initializations and processed video data for the period 2-5 September 1997. Video data were only available during daylight hours. SURF96 output was saved at 3-h intervals and linearly interpolated to 1-h intervals for comparison with video-derived data. Surf parameters have been averaged for each day and appear in bold. Because instrumentation was not available to measure parameters such as longshore current, this section presents a qualitative examination of the performance of SURF96.

##### *Average Wave Period*

Average wave period results from SURF96 showed some variability between initializations from STWAVE (SURF96-S) and REFDIF (SURF96-R). SURF96-S average wave period showed better agreement with video-derived data on 2 September, while SURF96-R was in general agreement on 3-4 September. Overall, SURF96-R compared more favorably with video data.

##### *Incident Wave Angle*

SURF96-R incident wave angles indicate a tendency for the waves to be directed between  $-10$  and  $-20^\circ$  toward the left flank. With the exception of positive values on 5 September, SURF96-S incident wave angles were generally in the range of  $-5$  to  $-15^\circ$ . An analysis of the deep-water WAM directional wave spectra input to STWAVE and REFDIF indicate that during the period 2-5 September, the peak directional wave energy is generally directed toward the left flank (negative). Figure 23(a) shows a contour plot of the deep-water spectral energy from WAM that was applied on the STWAVE outer boundary on 3 September at 15 GMT. Fig 23(b) shows the resulting energy density from STWAVE, which was used to force SURF96. In both cases, the maximum wave energy is directed toward the left flank (negative). However, refraction from STWAVE causes the waves to turn so they are more aligned with shore normal ( $330^\circ$ ). Higher resolution and more accurate wind forcing from improved models such as COAMPS could lead to better WAM initializations.

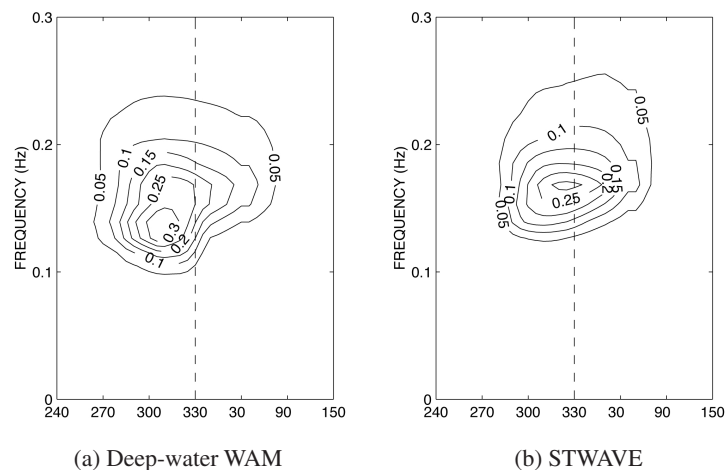


Fig. 23 – Directional wave spectra ( $\text{Hz}/\text{m}^2/\text{rad}$ ) on 3 September 1997 on Onslow Bay. Dashed line shows energy directed onto shore ( $330^\circ$ ).

Table 8 – Video-derived Data vs SURF96 Average Wave Period, Incident Wave Angle and Longshore Current Based on Initializations from REFDIF (REF) and STWAVE (STW)

<b>SURF Comparison vs Video Data</b>										
Date (1997)	Time (GMT)	Average Wave Period (s)			Incident Wave Angle (°)			Longshore Current (ms)		
		Video	REF	STW	Video	REF	STW	Video	REF	STW
02 Sep	1222	6.4	5.9	6.4	1.1	-13.4	-4.5	-0.26	-0.31	-0.18
	1313	7.5	5.5	6.0	4.0	-14.2	-7.7			
	1413	7.2	5.3	5.4	-3.0	-15.0	-11.0			
	1513	7.5	5.6	5.8	-6.1	-14.2	-10.6	-0.21	-0.26	-0.31
	1613	7.5	5.6	5.8				-0.06	-0.39	-0.44
<b>AVG</b>		<b>7.2</b>	<b>5.6</b>	<b>5.9</b>	<b>-1.0</b>	<b>-14.2</b>	<b>-8.5</b>	<b>-0.18</b>	<b>-0.32</b>	<b>-0.31</b>
03 Sep	0813	6.4	7.1	5.9	11.1	-9.3	-4.6	0.97	-0.15	-0.16
	0913	7.2	7.1	5.9	11.5	-9.6	-4.8	1.14	-0.15	-0.17
	1013	7.2	7.1	5.9	15.9	-9.9	-5.1	0.90	-0.15	-0.17
	1113	6.6	7.1	5.9	7.8	-10.1	-5.3	1.01	-0.15	-0.18
	1213	6.9	7.1	5.9	12.3	-10.2	-5.5	0.66	-0.20	0.13
	1313	7.2	7.1	5.9	34.0	-10.3	-4.7	0.30	-0.26	0.44
	1413	6.9	7.1	5.9	8.6	-10.4	-5.9			
	1513	6.6	7.3	5.9	8.9	-10.2	-5.5			
	1613	6.6	7.6	5.9	10.2	-10.0	-5.1	0.58	-0.31	0.74
	<b>AVG</b>		<b>6.8</b>	<b>7.2</b>	<b>5.9</b>	<b>13.4</b>	<b>-10.0</b>	<b>-5.3</b>	<b>0.79</b>	<b>-0.20</b>
04 Sep	0813	7.5	6.4	5.9	-3.2	-18.9	1.1	-0.79	-0.46	0.07
	0913	7.5	6.9	6.1	-3.8	-18.8	-4.3	-0.77	-0.44	-0.03
	1013	7.2	7.3	6.3	-20.1	-18.6	-9.6	-0.79	-0.43	-0.12
	1113	7.5	7.8	6.5	-4.2	-18.5	-15.0	-0.66	-0.41	-0.22
	1213	7.9	7.8	6.5	0.5	-19.5	-16.0	-0.77	-0.43	-0.24
	1313	7.5	7.8	6.5	0.3	-20.5	-17.0	-0.47	-0.44	-0.26
	1413	8.3	7.8	6.5	-4.0	-21.5	-18.0	-0.5	-0.46	-0.28
	1513	7.2	8.3	6.5	-23.3	-21.4	-17.3			
	<b>AVG</b>		<b>7.6</b>	<b>7.5</b>	<b>6.4</b>	<b>-7.2</b>	<b>-19.7</b>	<b>-12.0</b>	<b>-0.68</b>	<b>-0.44</b>
05 Sep	0713	7.5	10.3	8.2	-7.0	-19.4	9.8	-0.31	-0.50	0.29
	0813	9.7	10.3	6.5	-3.7	-18.9	18.7	-0.08	-0.41	0.45
	0913							-0.41	-0.37	0.36
	1008				-5.8	-18.0	16.8	-0.51	-0.34	0.28
	<b>AVG</b>		<b>8.6</b>	<b>10.3</b>	<b>7.4</b>	<b>-5.5</b>	<b>-18.8</b>	<b>15.1</b>	<b>-0.33</b>	<b>-0.41</b>

### *Longshore Current*

The direction in which the longshore current was oriented was in good agreement for both sets of hindcasts (SURF96-S and SURF96-R) on 2 and 4 September. Both models were in disagreement with video-derived data on 3 September. The longshore current is proportional to  $\sin \theta$ , where  $\theta$  represents the incident wave angle. Because  $\theta$  was negative for both sets of hindcasts, the longshore current is also negative. As discussed earlier, this is attributed to the WAM inputs. Due to the dependence of the longshore current on  $\sin \theta$ , larger values of  $\theta$  can result in greater longshore current magnitudes. The magnitude of the longshore current generally was within 25 to 75% of the magnitudes derived from video data. Overall, SURF96-R hindcasts showed reasonable agreement with video-based data on three out of the four days. SURF96-S showed comparable results to REFDIF on 2 and 4 September. The beach profile used in this study was obtained in April 1996, four months prior to Hurricane Fran, which hit the area. An updated beach profile may have contributed to more realistic results.

## 5. SUMMARY AND CONCLUSIONS

A suite of off-the-shelf wave, tide, and surf models were run in a hindcast mode as a coupled system near Onslow Beach to evaluate their performance. To evaluate the IOP suite of models, a series of oceanographic instruments were deployed in shallow water at Onslow Beach to measure wave heights, wave periods, and tidal elevations. One critical piece of the IOP modeling system is the wind forcing. In this evaluation, NORAPS wind speed and direction were used to drive WAM, ADCIRC, and STWAVE. Comparisons with available NDBC buoy data showed good agreement for NORAPS winds and WAM wave heights and periods. Underpredictions in wind speed led to lower wave heights from WAM, which in turn affected the shallow-water wave models STWAVE and REFDIF. A difference in wind direction by  $30^\circ$  for an extended period of time could also affect the propagation of waves. Overall, REFDIF and STWAVE compared generally well against in situ wave gauges. The correlation coefficients between gauge data and STWAVE model results averaged 0.74. Average STWAVE wave period was not as well correlated, however, RMS errors were less than 1 s. The other shallow-water wave model included in this study, REFDIF, performed nearly as well as STWAVE, although only one REFDIF location was examined in this study. ADCIRC tidal elevations were in very good agreement in phase and underestimated the amplitude by 14%. This is attributed to the accuracy and resolution of the wind forcing and the need for additional tidal constituents to be applied to the ADCIRC model boundary. The video-derived data showed reasonable comparison in SURF96 for wave period. The incident wave angle and longshore current agreed in direction for three out of the four days in which data were available. Magnitudes of the longshore current were generally within 25 to 75 cm/s of the video data. Planned future research will address issues regarding the differences between modeled vs observed breaker angles. Included in this work will be an examination of higher resolution and more accurate wind-forcing to remove some sources of error in the wave models.

In addition to improvements to wind-forcing for the deep-water WAM model, bathymetry can play an important role in the shallow-water wave models. The bathymetry used for the STWAVE and REFDIF hindcasts was collected prior to Hurricane Fran, which pummeled the coast near Onslow Beach in early September 1996. A more accurate bathymetry could yield more accurate results, especially in shallow water.

## 6. ACKNOWLEDGMENTS

This work was conducted under the sponsorship of the Ocean Executive Agent and the Defense Modeling and Simulation Office (DMSO). The authors thank Dr. Paul Farrar of NAVOCEANO for performing the WAM runs and providing WAM data; Dr. K. Todd Holland and Mr. Tim Kooney of the Mapping, Charting, and Geodesy Branch, Marine Geosciences Division, at NRL for collecting and processing the video imagery; Mr. Mark Hulbert of the Ocean Sciences Branch, Oceanography Division, for deploying and retrieving

instrumentation at Onslow Beach; Mr. C. Reid Nichols of the Marine Information Resources Corporation (MIRC), Ellicott City, Maryland (formerly of Neptune Sciences, Inc.) for processing the in situ data; Mr. Theodore Mettlach and Dr. Marshall Earle of Neptune Sciences, Inc., for REFDIF and SURF96 assistance; the U.S. Marine Corps Air Station at Camp Lejeune for providing hourly meteorological information, and the National Data Buoy Center for providing buoy data. The authors acknowledge the office of the Chief of Engineers, U.S. Army Corps of Engineers, for authorizing publication of this report.

## REFERENCES

1. R.A. Allard, Y.L. Hsu, M.J. Collins, J. McKee Smith, M. Earle, and K. Miles, "Use of Coupled Numerical Wave and Surf Models to Simulate the Littoral Environment from Deep Water to the Beach," NRL/FR/7322--98-9688, August 1998.
2. R.M. Hodur, "Evaluation of a Regional Model with an Update Cycle," *Mon. Wea. Rev.* **115**, 2707-2718 (1987).
3. WAMDI Group, "The WAM Model – A Third-Generation Ocean Wave Prediction Model," *J. Phys. Oceanogr.* **18**, 1775-1810 (1988).
4. G.J. Komen, L. Cavaleri, M. Donelan, K. Hasselmann, S. Hasselmann, and P.A.E.M. Janssen, *Dynamics and Modelling of Ocean Waves* (Cambridge University Press, Cambridge, U.K., 1994) pp. 532.
5. P.A. Wittmann and P.D. Farrar, "Global, Regional and Coastal Wave Prediction," *MTS J.* **31**, 76-82 (1997).
6. R.A. Luettich, J.J. Westerink, and N. Scheffner, "ADCIRC: An Advanced Three-Dimensional Circulation Model for Shelves, Coasts, and Estuaries, Report 1: Theory And Methodology Of ADCIRC-2DDI and ADCIRC-3DL," DRP-92-6, U.S. Army Engineer Waterways Experiment Station, Vicksburg, Miss., November 1992.
7. J.J. Westerink, C.A. Blain, R.A. Luettich and N. Sheffner, "ADCIRC: An Advanced Three-Dimensional Circulation Model for Shelves, Coasts, and Estuaries, Report 2: Users's Manual for ADCIRC-2DDI," DRP-92-6, U.S. Army Engineer Waterways Experiment Station, Vicksburg, Miss., January 1994.
8. J.J. Westerink, R.A. Luettich and N. Sheffner, "ADCIRC: An Advanced Three-Dimensional Circulation Model for Shelves, Coasts, and Estuaries, Report 3: Development of a Tidal Constituent Data Base for the Western Atlantic and Gulf of Mexico," DRP-92-6, U.S. Army Engineer Waterways Experiment Station, Vicksburg, Miss., June 1993.
9. D.T. Resio, "Shallow-Water Waves I: Theory," *J. Waterw. Port Coastal Ocean Eng. ASCE* **113**(3), 264-281 (1987).
10. D.T. Resio, "Shallow-Water Waves II: Data Comparisons," *J. Waterw. Port Coastal Ocean Eng. ASCE* **114**(1), 50-65 (1988).
11. J.M. Smith, D.T. Resio, and A.K. Zundel, "STWAVE: Steady-State Spectral Wave Model, Report 1: User's Manual for STWAVE Version 2.0," CHL-99-1, U.S. Army Engineer Waterways Experiment Station, Vicksburg, Miss., 1999.

12. J.T. Kirby and R.A. Dalrymple, "Combined Refraction (Diffraction Model REFDIF, Version 2.5, Documentation and User's Manual," Center For Applied Coastal Research, Univ. of Del., Report 94-22, 1994.
13. E.B. Thornton and R.T. Guza, "Transformation of Wave Height Distributions," *J. Geophys. Res.* **88**(C10), 5925-5938 (1983).
14. E.B. Thornton and R.T. Guza, "Surf Zone Longshore Currents and Random Waves: Field Data and Models," *J. Phys. Oceanogr.* **16**, 1165-1178 (1986).
15. L. Miguez, D. Osiecki, M. Earle, and T. Mettlach, "Software Design Document for the Oceanographic and Atmospheric Master Library, SURF 3.0 Forecasting Program," Neptune Sciences Inc., report for the Naval Oceanographic Office Systems Integration Department, February 1999.
16. C.R. Nichols and M.D. Earle, "Use of a Coupled Wave Buoy-Surf Model System to Support Combined Joint Task Force Exercise-96/Purple Star," Report for Center for Tactical Oceanographic Warfare Support Program Office, NRL, Stennis Space Center, Miss., May 1996.
17. K.T. Holland, R.A. Holman, T.C. Lippmann, J. Stanley, and N. Plant, "Practical Use of Video Imagery in Nearshore Oceanographic Field Studies," *IEEE J. Ocean Eng.* **22**(1), 81-92 (1997).